ChemPubSoc Europe

DOI: 10.1002/cbic.201700443

CHEMBIOCHEM Communications

Protonation-Initiated Cyclization by a Class II Terpene Cyclase Assisted by Tunneling

Adam Eriksson,[a] Charlotte Kürten,[b] and Per-Olof Syrén*[a, b]

Terpenes represent one of the most diversified classes of natural products with potent biological activities. The key to the myriad of polycyclic terpene skeletons with crucial functions in organisms from all kingdoms of life are terpene cyclase enzymes. These biocatalysts enable stereospecific cyclization of relatively simple, linear, prefolded polyisoprenes by highly complex, partially concerted, electrophilic cyclization cascades that remain incompletely understood. Herein, additional mechanistic light is shed on terpene biosynthesis by kinetic studies in mixed H_2O/D_2O buffers of a class II bacterial *ent*-copalyl diphosphate synthase. Mass spectrometry determination of the extent of deuterium incorporation in the bicyclic product, reminiscent of initial carbocation formation by protonation, resulted in a large kinetic isotope effect of up to seven. Kinetic analysis at different temperatures confirmed that the isotope effect was independent of temperature, which is consistent with hydrogen tunneling.

Terpenes are derived from the C5 precursor molecules dimethylallyl diphosphate (DMAPP) and isopentenyl diphosphate (IPP), which are fused by terpene synthase enzymes to yield elongated polyisoprenes. Subsequent cyclization of these relatively simple, linear building blocks by terpene cyclases enables the generation of a vast array of multicyclic molecular architectures,[1] with potent biological activities.[2] Stereospecific generation of tailored polycyclic terpenes provides access to chiral fine chemical synthons[3] and antifungal, -viral, -microbial, and -cancer agents.[2c,4] Bifunctional terpene synthases with distinct domains for linear terpene formation and cyclization have been described.[5] Terpene-synthesizing enzymes are classified according to the carbon content of their isoprene-derived substrate and are subdivided into mono- (C_{10}), sesqui- (C_{15}), di- (C_{20}), sester- (C_{25}), tri- (C_{30}), or tetra- (C_{40}) terpene cyclases. Bio-catalysts referred to as sesquarterpene cyclases that convert C_{35} isoprenoids were recently discovered.[1b] Enzyme-catalyzed cyclization is triggered by initial carbocation formation, either by cleavage of a terminal allylic diphosphate group (class I mechanism), or by aspartic acid catalyzed protonation of an isoprene or oxirane group of the prefolded substrate (class II mechanism, Scheme 1 A).[1] This onsets an electrophilic, partially concerted[6] ring-closure reaction cascade chaperoned by aromatic residues within the hydrophobic active site.[1] Termination of cyclization is achieved by quenching of the final carbocationic intermediate, through the addition of water or deprotonation by a suitable base.[7]

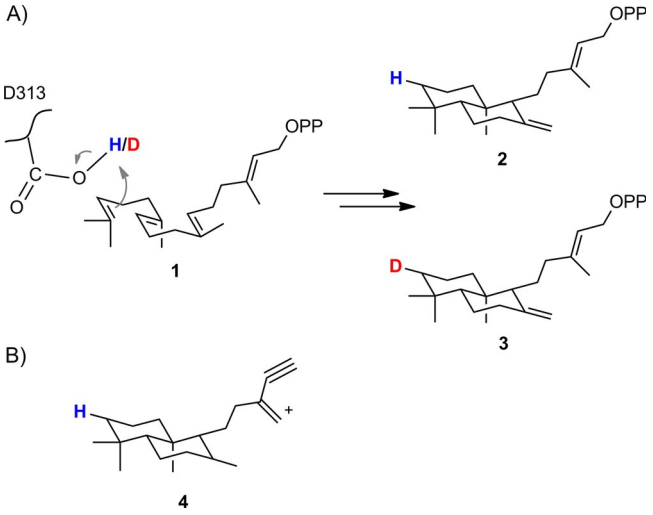

Scheme 1. Class II terpene cyclases initiate cyclization by protonation of a C=C isoprene (or oxirane) group of the prefolded substrate. A) Cyclization of geranylgeranyl diphosphate (**1**) by PtmT2 yields bicyclic *ent*-copalyl diphosphate. The possible incorporation of either hydrogen (blue, **2**) or deuterium (red, **3**) in the product is highlighted. The catalytic acid (D313) is also depicted. B) The mass fragment (**4**), corresponding to *m/z* 273, used in MS analysis of the extent of deuterium incorporation. The hydrogen atom originating from protonation by the catalytic acid is highlighted.

The complex reaction mechanisms displayed by terpene cyclases, which can involve hydride, methyl, and alkyl shifts[8] and/or ring expansion,[1] remain elusive.[1,5a] In particular, it has been postulated[9] that hydrogen tunneling[10] could be of importance for reaction mechanisms displayed by terpene biosynthetic machineries. We hypothesized that class II terpene cyclases that enable cyclization by a challenging protonation of nonactivated isoprenes—one that requires a catalytic acid residing in an unusual *anti* conformation[11]—would constitute suitable model systems to aid in resolving this mechanistic puzzle. We reasoned that kinetic analyses in mixed H_2O/D_2O

[a] *A. Eriksson, Prof. Dr. P.-O. Syrén*
School of Chemical Science and Engineering
KTH Royal Institute of Technology
100 44 Stockholm (Sweden)
E-mail: per-olof.syren@biotech.kth.se

[b] *C. Kürten, Prof. Dr. P.-O. Syrén*
Science for Life Laboratory, KTH Royal Institute of Technology
School of Biotechnology, Division of Proteomics
171 21 Stockholm (Sweden)

Supporting information and the ORCID identification numbers for the authors of this article can be found under https://doi.org/10.1002/cbic.201700443.

buffers coupled with mass spectrometry would allow for determination of intrinsic[10,12] kinetic isotope effects (KIEs), without the need for radioactive isotopes or labeled substrates. Thus, we turned our attention towards *ent*-copalyl diphosphate synthase from *Streptomyces platensis* (PtmT2);[13] a soluble bacterial diterpene cyclase that generates a bicyclic scaffold from **1** (Scheme 1 A). Substrate conversion by this biocatalyst could readily be followed by HPLC and UV detection (Figure S1 in the Supporting Information). Analysis of the corresponding fragmentation pattern of the product, following electrospray ionization, identified a suitable fragment (**4**, Scheme 1 B) with high intensity (Figure S2) that could act as a potential probe for incorporation of hydrogen or deuterium. Enzyme incubation in heavy water (i.e., 94% D_2O buffer, pD 6, 28 °C) showed a shift in mass and relative intensity of the fragment signal from *m/z* 273 to 274, as expected (Figure S3). Analysis of relative signal intensities and correcting for the relative abundancy of deuterium in the buffer [see Eq. (4) in the Experimental Section] resulted in a large KIE of seven. Although a KIE of seven is not significantly larger than that expected for classical proton transfers,[12b] primary KIEs of this magnitude have, in some cases, been found to be associated with tunneling in chemistry[14] and enzymology.[15] At 94% D_2O, small differences in buffer composition due to experimental error will affect the ratio of relative abundance of deuterium over hydrogen significantly. This potential source of error in $[D_2O]/[H_2O]$ was addressed by measuring the KIE in mixed H_2O/D_2O buffers of the same acidic strength (i.e., pH and pD of 6), for several additional relative concentrations of deuterium (i.e., 24, 48, 72%; the lower value chosen to reduce experimental error associated with analysis of MS signal intensity). The KIE at 28 °C converged to 4 under these experimental conditions (Table S1). Because the magnitude of the measured KIE does not directly confirm hydrogen tunneling,[12b] the temperature dependence of the KIE was determined. Competition experiments demonstrated that the KIE was essentially independent of temperature under our experimental conditions (Figure 1, temperature range 7–30 °C). Such temperature-independent KIEs have been observed for several biocatalytic systems[12,16] and are considered to be an important characteristic of enzyme-mediated hydrogen tunneling.[10,12b,16b] Because the isotope effect was essentially independent of temperature, Arrhenius analysis was performed based on the average values of the isotope effect over the investigated temperature range and for each D_2O concentration (Figure 1 B). The ratio of associated pre-exponential factors, A_H and A_D, converged to around four for the lower relative concentrations of deuterium (Table 1). A_H/A_D ratios separated from one are in accordance with hydrogen tunneling in enzymes and ratios of four have previously been observed for several biocatalytic systems that mediate hydrogen transfer "through the barrier".[12b]

Table 1. Pre-exponential Arrhenius factors obtained by analysis of the temperature dependence of the KIE.[a]

D_2O [%]	24	48	72	94
A_H/A_D[b]	4.4 ± 0.5[c]	3.9 ± 0.3[c]	4.2 ± 0.4[c]	6 ± 2[c]

[a] The investigated temperature range was from 7 to 30 °C, at pH and pD of 6, see the Experimental Section. [b] Values shown are based on Arrhenius analysis of the four data series (i.e., 24, 48, 72, and 94% D_2O) shown in Figure 1, by using the average values of the isotope effect to determine A_H/A_D. For 24 and 48% D_2O, forced fitting of the data as a linear function of $1/T$ resulted in A_H/A_D of 5 and 4, respectively (with slopes corresponding to $\Delta_{H\text{-}D}E_a$ of 60 and 20 cal mol^{-1}, respectively). [c] Estimated error range based on 2% uncertainty in pipetting.

Kinetic analysis of PtmT2 in both light and heavy water confirmed that experiments were performed under substrate-saturating conditions, and further revealed complex overall solvent isotope effects on macroscopic rate constants (Table S2). The approximatively twofold reduction of $k_{cat.}$ in heavy water is consistent with initial protonation significantly contributing to the rate-limiting step, according to Equation (1):

$$\frac{1}{k_{cat,obs}} = \frac{1}{k_{prot}} + \frac{1}{k_{other}} \quad (1)$$

in which $k_{cat,obs}$ corresponds to the observed overall macroscopic rate constant, k_{prot} to the rate constant for proton transfer accessed by mass spectrometry, and k_{other} to additional contributions to the barrier.

To further support the observed temperature independence of the KIE and associated small difference in activation energy for transfer of H versus D, an in silico model of the initial protonation step catalyzed by PtmT2 was constructed (Figure 2).

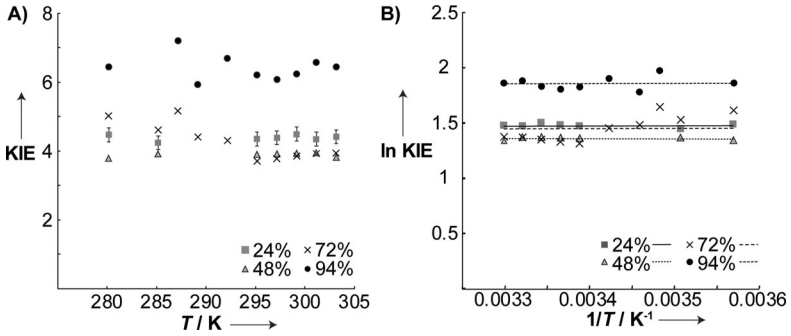

Figure 1. Temperature dependence of the KIE, as measured by MS at different concentrations of heavy water. A) KIE plotted as a function of temperature. Error bars are shown for the lower concentration of D_2O (i.e., 24%). B) Arrhenius analysis of the temperature dependence of the KIE. The lines shown correspond to average values of the isotope effect over the whole temperature range for each concentration of D_2O.

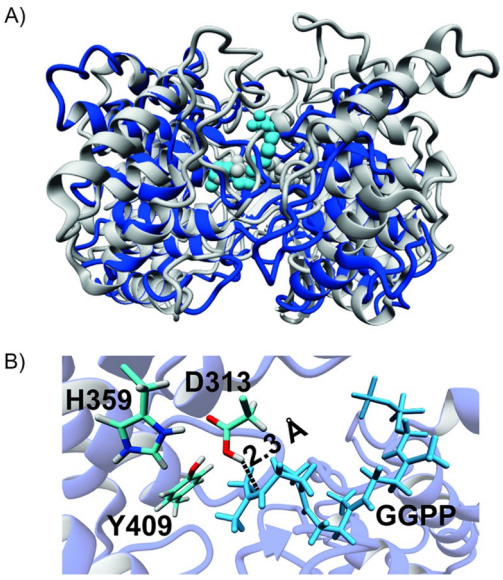

Figure 2. Structure and molecular modeling of PtmT2. A) Superposition of the diterpene cyclase from *S. platensis* (blue, PDB 5BP8,[13] with modeled substrate **1** shown in light-blue balls) and the triterpene cyclase from *A. acidocaldarius* (gray, PDB ID: 1UMP,[18] with the cocrystallized substrate analogue depicted in gray balls), showing the common $(\alpha/\alpha)_6$ barrel fold of class II terpene cyclases. Overall, the root-mean-square deviation (RMSD) was 2.1 Å. B) Energy-minimized snapshot of protonation-initiated cyclization by PtmT2. The catalytic amino acid (D313) and two adjacent amino acids are shown. Prefolded substrate **1** is shown in blue sticks.

This basal model for juxtaposition of the substrate in the available crystal structure of the empty enzyme does not account for effects of the "heavy" deuterated enzyme, which could influence protein motions.[17] Force field minimization of the biocatalyst complexed with the natural and prefolded substrate (Figure 2B) unraveled a distance for protonation of 2.3 Å, which was significantly less than that of the corresponding van der Waals value of 2.9 Å. In analogy, a protonation distance of 3.2 Å for the corresponding heavy atoms has been suggested based on analysis by AutoDock.[13] Molecular dynamics (MD) simulations of the triterpene cyclase from *Alicyclobacillus acidocaldarius*, which also operates by the class II mechanism and displays the same fold as that of PtmT2 (Figure 2A), have shown that very short protonation distances down to 1.7 Å are feasible.[19] Compressed internuclear distances have been attributed to "tunnel-ready" conformations.[12b]

Terpenes comprise the largest and most diversified class of natural products, with important biochemical functions in providing cell membrane rigidity, defense, and signaling.[1] Because terpenes constitute a large pool of sustainable biobricks, the generation of chiral and renewable terpene-based fine chemicals by biocatalytic[20] and metabolic engineering efforts[21] currently receive significant attention. Recently, focus has been on diterpene cyclases for synthetic applications[22] and enhanced understanding of fundamental metabolism.[2b] The class II *ent*-copalyl diphosphate synthase from *S. platensis*[13] (PtmT2) investigated herein harbors a β,γ-fold reminiscent of triterpene cyclases (Figure 2A) that act on nonphosphorylated C_{30} substrates. Thus, the catalytic mechanism of PtmT2 could possibly have originated from an ancestral triterpene cyclase and is therefore of considerable evolutionary interest.[23] Apart from applications as fine-chemical synthons, terpenes/terpenoids constitute valuable monomers for the generation of advanced sustainable polymers;[24] potent biofuels;[25] flavors and fragrances;[3a] medicines, including anticancer compounds already on the market, such as taxol;[26] or as new leads in cancer chemotherapy, such as fusicoccin A.[5a] Expanding our present incomplete understanding of fundamental terpene biochemistries would thus be beneficial in several scientific fields.[5a] Herein, by capitalizing on competition experiments and MS analysis of the extent of incorporation of H or D into the product, we provide, to the best of our knowledge, the first experimental evidence that supports hydrogen tunneling in terpene cyclases. The fact that proton transfers in the context of tunneling are typically associated with smaller isotope effects than those of hydrogen, or hydride migrations, has been discussed.[12b] It is likely that deuterium incorporation into the protein backbone affects other rate constants than that of protonation. This is perhaps well illustrated by an experimentally determined twofold increase in k_{cat}/K_M in heavy water relative to that in light water (Table S2). Dynamic effects have been suggested to assist terpene biosynthesis by modulating product distribution[27] and by shielding reactive carbocationic intermediates from water.[28] Based on pre-steady-state kinetics, product release has been suggested to constitute the rate-limiting step for class I terpene cyclases.[29] Our results do not exclude significant contribution of protein dynamics to the rate-limiting step.

In addition to substrate prefolding[6b] and initiation of cyclization, proton transfers and/or hydride shifts play important roles in determining the outcome of biological polycyclization cascades.[8] Thus, enzyme-assisted tunneling, potentially facilitated by the inherent "plastic" nature of terpene cyclases,[30] could be of importance in various terpene biosynthetic mechanisms.

Experimental Section

Transformation, protein expression, and purification: The PtmT2 gene from *S. platensis* (UniProtKB accession code A0A023VSF1, amino acid sequence 1–533) fused to an N-terminal His_6 tag in a pet22b+ plasmid, was expressed in *Escherichia coli* BL21 (DE3). An aliquot of an overnight culture was transferred into 2xYT-Amp (300 mL; 16 g L^{-1} tryptone, 10 g L^{-1} Yeast extract, 5 g L^{-1} NaCl, 100 mg L^{-1} ampicillin) to reach an OD_{600} of 0.07 and shaken at 37 °C, 160 rpm until OD_{600} = 0.6. Expression was induced by addition of isopropyl β-D-1-thiogalactopyranoside (IPTG; 0.25 mM) and was performed at 18 °C overnight at 160 rpm. The cells were harvested by centrifugation (7650 *g*, 10 min, 4 °C; Thermo Scientific Sorvall ST 16R). Cells were resuspended in lysis buffer (3 mL g^{-1} wet-weight; 100 mM Tris, 200 mM NaCl, 15 mM imidazole, 10% glycerol, pH 7.8) and sonicated three times (pulse 1 s on 1 s off, total time 50 s, amplitude 80%). The lysed cells were centrifuged (Beckman Coulter Avanti J-26 XP; 39200 *g*, 35 min, 4 °C), the supernatant was added to Ni-NTA agarose beads (1.5 mL, Qiagen) and incubated for 1 h with end-over-end shaking on ice. The beads were washed with lysis buffer (2×10 mL). PtmT2 was eluted with elution buffer (10×1 mL; 150 mM Tris, 100 mM NaCl, 300 mM imi-

dazole, 10% glycerol, pH 7.8). The fractions containing pure PtmT2, as determined by SDS-PAGE (Figure S4), were transferred to a centrifugal filter (Amicon Ultra-15, PLTK Ultracel-PL) with a molecular weight cutoff (MWCO) of 30 kDa for concentration, desalting, and buffer exchange to storage buffer (50 mM Tris, 100 mM NaCl, 50 mM KCl, 5% glycerol, pH 7.8). Obtained PtmT2 was stored at 4 °C. Protein concentration was determined by using BradfordUltra (Expedeon) with bovine serum albumin (BSA) as reference.

Kinetic and isotope effect analyses: Kinetic parameters of PtmT2 were determined by measuring the conversion of its substrate **1** (≥95% in 7:3 MeOH/NH_4OH; Sigma–Aldrich) to the product *ent*-copalyl diphosphate at different time points. All kinetic assays were performed in kinetic buffer (50 mM citric acid, 1 mM $MgCl_2$, 1 mM β-mercaptoethanol, 10% glycerol, pH 6.0), with PtmT2 (20 nM) and various concentrations of **1** (10, 15, 20, 25, 30, 50, 100, 150, and 200 μM) in a total volume of 100 μL. The reaction mixtures were incubated at 30 °C, and different reaction times (1, 3, 5, and 7 min) were chosen, at which methanol (100 μL) was added to quench the reaction. The reaction mixtures were analyzed by means of HPLC on an Agilent Technologies 1100 HPLC system, coupled with an ESI mass spectrometer. HPLC analysis was performed by using a 50×3.0 mm C_{18} column, 6 min run time, a flow of 1 mL min^{-1}, and a solvent gradient of 10–97% acetonitrile in NH_4OH (10 mM). The product was detected by UV analysis at $\lambda = 215$ nm.

Similar experiments were performed for D_2O (heavy water, 99 atom%; Sigma–Aldrich) by using kinetic buffer (50 mM citric acid, 1 mM $MgCl_2$, 1 mM β-mercaptoethanol, 10% glycerol, D_2O, pD 6.0). The pD value was set according to Equation (2)[31] to obtain the corresponding acidic strengths in H_2O and D_2O:

$$pD = pH + 0.40 \quad (2)$$

Due to a reduction in K_M in D_2O, lower concentrations of **1** (5, 10, 15, 20, 25, 30, 50, 100, and 150 μM) were used. The three exchangeable protons per molecule of glycerol were considered when calculating the deuterium content in the kinetic buffer and in the reaction mixture. This led to a maximum D_2O concentration of 94%. The effect of citric acid was negligible.

Michaelis–Menten Equation (3) was used to determine $k_{cat.}$ and K_M values by using the least-squares method in Excel.

$$V_0 = k_{cat.}[E]_0 \frac{[S]}{K_M + [S]},\ [E]_0 \ll [S] \quad (3)$$

For isotope effect analysis, reaction times of 10 min to 3 h at different temperatures (7.0, 12.0, 14.0, 16.0, 19.0, 22.0, 24.0, 26.0, 28.0, and 30.0 °C) and D_2O concentrations (0, 24, 48, 72, and 94%) were used with 0.2 μM PtmT2 and 100 μM **1**. The KIE (i.e., k_H/k_D) was determined by MS analysis of the ratio of relative intensities between protonated and deuterated product fragments (Scheme 1B) by using Equation (4):[32]

$$KIE = \frac{k_H}{k_D} = \frac{1}{1/R_{obs} - 1/R_0} \times \frac{D_2O\,\%}{H_2O\,\%} \quad (4)$$

$$R_{obs} = \frac{I_{light}}{I_{heavy}} \quad (5)$$

$$R_0 = \left(\frac{I_{light}}{I_{heavy}}\right)_{H_2O} \quad (6)$$

R_{obs} corresponds to the measured fraction of protonated over deuterated product [Eq. (5)]; R_0 to the measured natural isotope distribution in light water [Eq. (6)]; and D_2O% and H_2O% to the relative distributions of deuterium atoms and protons in the solution, respectively. Reported KIEs were averages based on two to five independent measurements.

The ratio of pre-exponential factors (A_H/A_D) was determined as the average value of the KIE based on temperature independence and according to the linear Arrhenius Equation (7):

$$\ln KIE = \ln \frac{k_H}{k_D} = -\frac{E_{a_H} - E_{a_D}}{R} \frac{1}{T} + \ln \frac{A_H}{A_D} \quad (7)$$

in which E_{aH} and E_{aD} correspond to the activation energy for transfer of a proton and deuterium, respectively.

Molecular modeling: The PDB structure 5BP8[13] of PtmT2 without substrate was used for the computational analysis in YASARA,[33] with the aim of generating a model of a biocatalyst complexed with prefolded substrate. Co-crystallized ligands were removed and, for optimal modeling and positioning of substrate **1** in the active site, the structure was superposed onto the class II triterpene cyclase from *A. acidocaldarius* (PDB ID: 1UMP[18]) containing a substrate analogue in its active site. The substrate analogue was transferred to the PtmT2 active site and remodeled to **1**. Hydrogen atoms were added and adequate protonation states were obtained by setting the pH to 6, by using YASARA. Force field parameters for **1** were obtained by the AutoSMILES approach, as implemented in YASARA.[33] Energy minimization was performed by using the AMBER14 force field and standard settings in YASARA (i.e., PME for long-range electrostatics, a cutoff for nonbonding interactions of 8 Å, periodic boundary conditions). After a short MD simulation (5 ps, 298 K), followed by energy minimization, the distance between the proton residing at the catalytic D313 in the conserved DDXD motif[1] and the proton acceptor in **1** was determined.

Acknowledgements

Support from the Swedish Research Council, Young Investigator grant 621-2013-5138, ÅForsk Foundation grant 17-359, and the PDC Center for High Performance Computing at the Royal Institute of Technology (KTH) is greatly acknowledged. We thank Birger Sjöberg and Ylva Gravenfors at the Science for Life Laboratory for support with the LC/MS measurements.

Conflict of Interest

The authors declare no conflict of interest.

Keywords: biosynthesis · enzyme catalysis · isotope effects · kinetics · reaction mechanisms

[1] a) E. Oldfield, F.-Y. Lin, *Angew. Chem. Int. Ed.* **2012**, *51*, 1124–1137; *Angew. Chem.* **2012**, *124*, 1150–1163; b) T. Sato, S. Yoshida, H. Hoshino, M. Tanno, M. Nakajima, T. Hoshino, *J. Am. Chem. Soc.* **2011**, *133*, 9734–9737.

[2] a) C. J. Schwalen, X. Feng, W. Liu, B. O-Dowd, T.-P. Ko, C. J. Shin, R.-T. Guo, D. A. Mitchell, E. Oldfield, *ChemBioChem* **2017**, *18*, 985–991; b) R. S. Nett, M. Montanares, A. Marcassa, X. Lu, R. Nagel, T. C. Charles, P. Hedden, M. C. Rojas, R. J. Peters, *Nat. Chem. Biol.* **2017**, *13*, 69–74; c) S. Mafu, P. S. Karunanithi, T. A. Palazzo, B. L. Harrod, S. M. Rodriguez, I. N.

Mollhoff, T. E. O'Brien, S. Tong, O. Fiehn, D. J. Tantillo, J. Bohlmann, P. Zerbe, *Proc. Natl. Acad. Sci. USA* **2017**, *114*, 974 – 979.
[3] a) M. Schalk, L. Pastore, M. A. Mirata, S. Khim, M. Schouwey, F. Deguerry, V. Pineda, L. Rocci, L. Daviet, *J. Am. Chem. Soc.* **2012**, *134*, 18900 – 18903; b) X. Tang, R. K. Allemann, T. Wirth, *Euro. J. Org. Chem.* **2017**, *2017*, 414 – 418.
[4] C.-J. Zhang, J. Wang, J. Zhang, Y. M. Lee, G. Feng, T. K. Lim, H.-M. Shen, Q. Lin, B. Liu, *Angew. Chem. Int. Ed.* **2016**, *55*, 13770 – 13774; *Angew. Chem.* **2016**, *128*, 13974 – 13978.
[5] a) M. Chen, W. K. Chou, T. Toyomasu, D. E. Cane, D. W. Christianson, *ACS Chem. Biol.* **2016**, *11*, 889 – 899; b) A. C. Huang, S. A. Kautsar, Y. J. Hong, M. H. Medema, A. D. Bond, D. J. Tantillo, A. Osbourn, *Proc. Natl. Acad. Sci. USA* **2017**, *114*, E6005 – E6014.
[6] a) L. Smentek, B. A. Hess, Jr., *J. Am. Chem. Soc.* **2010**, *132*, 17111 – 17117; b) R. Rajamani, J. Gao, *J. Am. Chem. Soc.* **2003**, *125*, 12768 – 12781.
[7] a) K. U. Wendt, A. Lenhart, G. E. Schulz, *J. Mol. Biol.* **1999**, *286*, 175 – 187; b) K. C. Potter, J. C. Zi, Y. J. Hong, S. Schulte, B. Malchow, D. J. Tantillo, R. J. Peters, *Angew. Chem. Int. Ed.* **2016**, *55*, 634 – 638; *Angew. Chem.* **2016**, *128*, 644 – 648.
[8] D. J. Tantillo, *Nat. Prod. Rep.* **2011**, *28*, 1035 – 1053.
[9] D. T. Major, Y. Freud, M. Weitman, *Curr. Opin. Chem. Biol.* **2014**, *21*, 25 – 33.
[10] J. Meisner, J. Kaestner, *Angew. Chem. Int. Ed.* **2016**, *55*, 5400 – 5413; *Angew. Chem.* **2016**, *128*, 5488 – 5502.
[11] R. D. Gandour, *Bioorg. Chem.* **1981**, *10*, 169 – 176.
[12] a) A. R. Offenbacher, S. Hu, E. M. Poss, C. A. M. Carr, A. D. Scouras, D. M. Prigozhin, A. T. Iavarone, A. Palla, T. Alber, J. S. Fraser, J. P. Klinman, *ACS Cent. Sci.* **2017**, *3*, 570 – 579; b) J. P. Klinman, *J. Phys. Org. Chem.* **2010**, *23*, 606 – 612; c) J. P. Klinman, A. Kohen, *Annu. Rev. Biochem.* **2013**, *82*, 471 – 496.
[13] J. D. Rudolf, L. B. Dong, H. Cao, C. Hatzos-Skintges, J. Osipiuk, M. Endres, C. Y. Chang, M. Ma, G. Babnigg, A. Joachimiak, G. N. Phillips, Jr., B. Shen, *J. Am. Chem. Soc.* **2016**, *138*, 10905 – 10915.
[14] M. J. S. Dewar, E. F. Healy, J. M. Ruiz, *J. Am. Chem. Soc.* **1988**, *110*, 2666 – 2667.
[15] D. G. Truhlar, J. Gao, C. Alhambra, M. Garcia-Viloca, J. Corchado, M. L. Sanchez, J. Villa, *Acc. Chem. Res.* **2002**, *35*, 341 – 349.
[16] a) P. Hothi, S. Hay, A. Roujeinikova, M. J. Sutcliffe, M. Lee, D. Leys, P. M. Cullis, N. S. Scrutton, *ChemBioChem* **2008**, *9*, 2839 – 2845; b) A. Kohen, *Acc. Chem. Res.* **2015**, *48*, 466 – 473; c) L. Masgrau, A. Roujeinikova, L. O. Johannissen, P. Hothi, J. Basran, K. E. Ranaghan, A. J. Mulholland, M. J. Sutcliffe, N. S. Scrutton, D. Leys, *Science* **2006**, *312*, 237 – 241.
[17] L. Y. P. Luk, J. J. Ruiz-Pernia, A. S. Adesina, E. J. Loveridge, I. Tunon, V. Moliner, R. K. Allemann, *Angew. Chem. Int. Ed.* **2015**, *54*, 9016 – 9020; *Angew. Chem.* **2015**, *127*, 9144 – 9148.
[18] K. U. Wendt, K. Poralla, G. E. Schulz, *Science* **1997**, *277*, 1811 – 1815.
[19] S. C. Hammer, P.-O. Syren, B. Hauer, *ChemistrySelect* **2016**, *1*, 3589 – 3593.
[20] S. C. Hammer, A. Marjanovic, J. M. Dominicus, B. M. Nestl, B. Hauer, *Nat. Chem. Biol.* **2015**, *11*, 121 – 126.
[21] J. Andersen-Ranberg, K. T. Kongstad, M. T. Nielsen, N. B. Jensen, I. Pateraki, S. S. Bach, B. Hamberger, P. Zerbe, D. Staerk, J. Bohlmann, B. L. Møller, B. Hamberger, *Angew. Chem. Int. Ed.* **2016**, *55*, 2142 – 2146; *Angew. Chem.* **2016**, *128*, 2182 – 2186.
[22] Y.-l. Yang, S. Zhang, K. Ma, Y. Xu, Q. Tao, Y. Chen, J. Chen, S. Guo, J. Ren, W. Wang, Y. Tao, W.-B. Yin, H. Liu, *Angew. Chem. Int. Ed.* **2017**, *56*, 4749 – 4752; *Angew. Chem.* **2017**, *129*, 4827 – 4830.
[23] M. J. Smanski, R. M. Peterson, S.-X. Huang, B. Shen, *Curr. Opin. Chem. Biol.* **2012**, *16*, 132 – 141.
[24] Y. Zhu, C. Romain, C. K. Williams, *Nature* **2016**, *540*, 354 – 362.
[25] P. P. Peralta-Yahya, F. Zhang, C. S. B. del, J. D. Keasling, *Nature* **2012**, *488*, 320 – 328.
[26] B. A. Weaver, *Mol. Biol. Cell* **2014**, *25*, 2677 – 2681.
[27] D. T. Major, M. Weitman, *J. Am. Chem. Soc.* **2012**, *134*, 19454 – 19462.
[28] Y. Gao, R. B. Honzatko, R. J. Peters, *Nat. Prod. Rep.* **2012**, *29*, 1153 – 1175.
[29] a) J. R. Mathis, K. Back, C. Starks, J. Noel, C. D. Poulter, J. Chappell, *Biochemistry* **1997**, *36*, 8340 – 8348; b) D. E. Cane, H.-T. Chiu, P.-H. Liang, K. S. Anderson, *Biochemistry* **1997**, *36*, 8332 – 8339.
[30] B. T. Greenhagen, P. E. O'Maille, J. P. Noel, J. Chappell, *Proc. Natl. Acad. Sci. USA* **2006**, *103*, 9826 – 9831.
[31] P. K. Glasoe, F. A. Long, *J. Phys. Chem.* **1960**, *64*, 188 – 190.
[32] P.-O. Syrén, S. C. Hammer, B. Claasen, B. Hauer, *Angew. Chem. Int. Ed.* **2014**, *53*, 4845 – 4849; *Angew. Chem.* **2014**, *126*, 4945 – 4949.
[33] E. Krieger, T. Darden, S. B. Nabuurs, A. Finkelstein, G. Vriend, *Proteins Struct. Funct. Bioinf.* **2004**, *57*, 678 – 683.

Manuscript received: August 18, 2017
Accepted manuscript online: October 5, 2017
Version of record online: November 3, 2017

